JOURNAL GEOLOGICAL SOCIETY OF INDIA
Vol.97, March 2021, pp.315-325

Geochemical Characteristics of Quartzite in Parts of Paleo-proterozoic Dhanjori Group, Singhbhum Craton, Eastern India: Implications for Provenance and Paleoweathering

Usman Aarif Chaudhary* and Shabber Habib Alvi
Department of Geology, Aligarh Muslim University, Aligarh - 202 002, India
***E-mail:** *usman4851@gmail.com*

ABSTRACT

Singhbhum craton preserves the records of sedimentation, magmatism, and tectono-thermal events from Mesoarchaean to Neoproterozoic. The Dhanjori Group (DG), located on the north-east margin of the Singhbhum craton, comprises of a variety of rocks including quartz pebble conglomerate, quartzite, schist, inter-layered with mafic to intermediate and rarely acidic lava flows, tuff and agglomerate. Petrography and geochemical characteristics of the Dhanjori quartzite have been undertaken to interpret paleoweathering and provenance characteristics. Studied quartzites are made up of abundant quartz, feldspar, mica, and lithic fragments. With the help of geochemical data, the studied quartzites are classified as quartz-arenites and sub-arkoses. In addition to the A-CN-K plot, various chemical indices such as the chemical index of weathering (CIW), chemical index of alteration (CIA), and plagioclase index of alteration (PIA) indicate moderate to intense chemical weathering of the provenance under semi-humid climatic conditions. Rare earth element (REE) chondrite normalized patterns of the studied samples illustrate enriched light rare earth elements (LREEs) (La_N/Sm_N = 3.11 – 6.19), depleted heavy rare earth elements (HREEs) (Gd_N/Yb_N = 0.35 – 3.12) and negative Eu anomaly (Eu/Eu* = 0.55 - 0.87, ~ 0.68). Such patterns are similar to that of the upper continental crust (UCC). In the discrimination function diagram, studied samples of the Dhanjori Group fall in quartzose sedimentary field. In addition, La/Sc vs. Th/Co and La-Th-Sc diagrams, various ratios like Th/Sc (~0.61), La/Sc (~4.42), Th/Co (~0.03), La/Co (~0.11), and Cr/Th (~141.62) imply a mixed provenance for the studied samples. Hence, it has been inferred that the meta-sediments and ortho-amphibolites of the older metamorphic group, Singhbhum granitoid complex, as well as associated Archaean metavolcanic suites, would have acted as the probable source rocks for the studied Dhanjori quartzites.

INTRODUCTION

Singhbhum craton (SC) (Fig.1) is one of the world's few Precambrian terrains that exhibit volcanism and sedimentation ranging in age from the Paleoarchaean to Neoproterozoic (Prabhakar and Bhattacharya, 2013; Nelson et al., 2014, De et al., 2015; Olierook et al., 2019). The SC reveals a large tract of Precambrian rocks covering about 50,000 km^2 areas. In the SC, from south to north, three different petrotectonic zones have been recognized: (1) southern Archaean nucleus composed of iron formations, granitoids, Neoarchaean sedimentary formations (Mazumder et al., 2012) and newer dolerite dykes (Saha, 1994; Mir et al., 2011a, b; Mir and Alvi, 2015), (2) North Singhbhum mobile belt, made up of Chandil, Dhalbhum, Dalma, Chaibasa formations, and Dhanjori Group (Gupta and Basu, 2000; Alvi et al., 2019), (3) Chotanagpur granite gneissic complex (CGGC) made up of migmatites, granites, gneisses, etc. The DG is considered as younger to the Singhbhum Group (SG), by Dunn and Dey (1942) and in the revised stratigraphic succession of Saha (1994). However, many other workers believe that the DG is older to the SG (Mukhopadhyay, 1976; Basu, 1985; Gupta et al. 1985). The SC, an Archaean craton of the Indian shield, conserves sedimentary records of Mesoarchaean to Neoproterozoic period; however, geochemical studies on sedimentary formations and relating to Archaean upper crust composition are scarce. The earlier research works have been carried out to assess sedimentological and stratigraphic studies of the DG (e.g. Mazumder and Sarkar, 2004; Mazumder, 2005; Bhattacharya and Mahapatra, 2008; Mazumder et al., 2012; De et al., 2015). Hence, the objective of the current work is to determine the provenance and source area weathering characteristics of the quartzites of the Paleoproterozoic Dhanjori Group. Such geochemical studies of the Dhanjori Group of rocks may play a vital role in understanding the early post-Archaean evolution of the Dhanjori Group and the evolution of the Singhbhum craton.

GEOLOGICAL SETTING

The DG covers an area of around 800 km^2, contains sedimentary, volcanic, and volcaniclastic rocks and show low grade green-schist facies metamorphism (Gupta et al., 1985; Basu, 1985; Singh and Nim, 1998). The DG extends from Singpura to Narwapahar in the east-west direction and dips towards the north (Fig.2). The DG lies unconformably over the Archaean nucleus and is conformably overlain by the Chaibasa Formation (Mukhopadhyay, 1976; Mazumder et al., 2015; De et al., 2015). It comprises of siliciclastic, mafic to minor felsic volcanic, and volcanoclastic rocks (De et al., 2015). Researchers like Dunn and Dey (1942), Sarkar and Saha (1983) believed that the DG is younger to the Chaibasa Formation, whereas Sarkar and Deb (1971) and Mukhopadhyay (1976) stated that the normal stratigraphic order is shown by the Dhanjori and Chaibasa successions. However, occurrences of 3.04-3.09 Ga old (Acharyya et al., 2010) U bearing quartz-pebble-Cconglomerate at the bottom of the Dhanjori meta-sediments (Sunil Kumar et al., 1998), Pb-Pb WR isochron ages of 2858 ± 17; 2749 ± 210 Ma obtained for the Dhanjori metavolcanic rocks (Mishra and Johnson, 2005) and Sm-Nd T_{DM} model ages of 2460, 2498, 2517, 2519 Ma obtained for soda granitoids (Pandey et al., 1986) perhaps points towards the older age of the Dhanjori Group, which corroborates the observation of Mukhopadhyay (1976, 1988). The Dhanjori Group is made of the lower formation (contains quartzites, phyllites, schist, and conglomerate) and upper formation (contains volcanic rocks, volcanoclastic rocks, quartzites, and phyllites) (Gupta et al., 1985).

METHODOLOGY

Studied samples of the Dhanjori Group were collected randomly

0016-7622/2021-97-3-315/$ 1.00 © GEOL. SOC. INDIA | DOI: 10.1007/s12594-021-1683-5

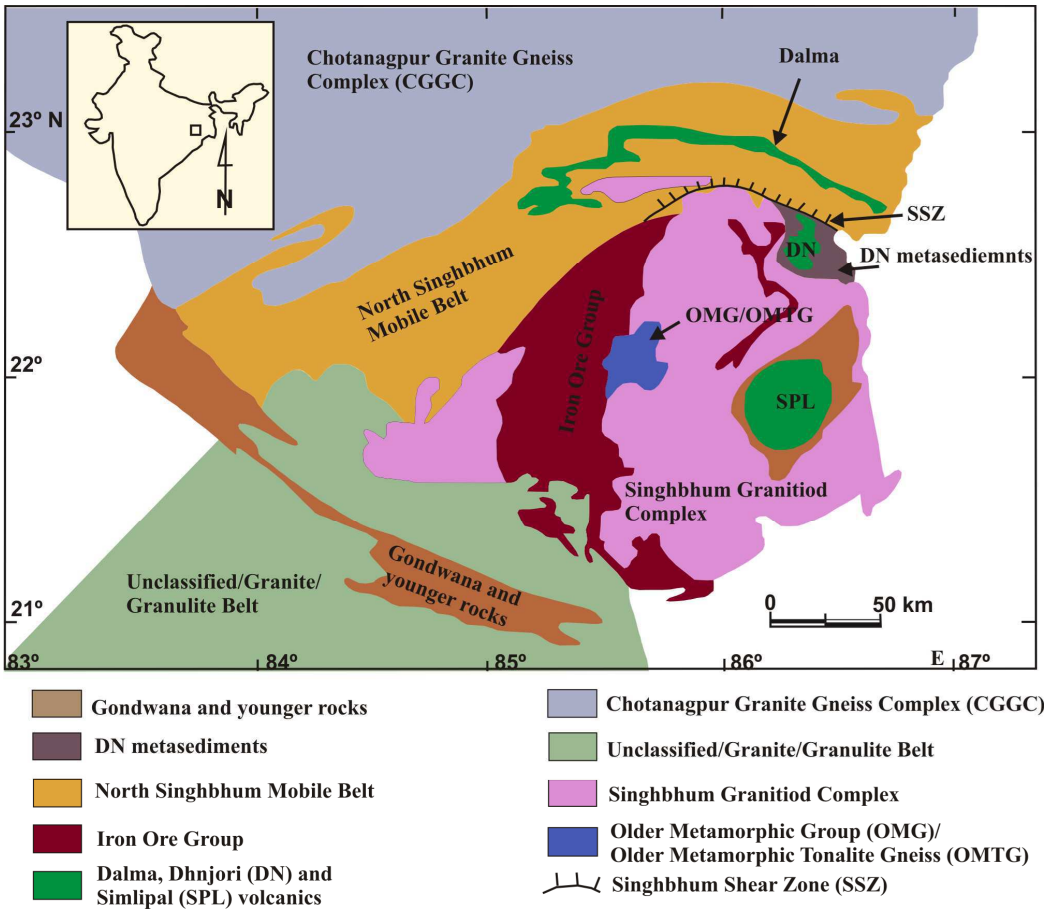

Fig.1. Geological map of the Singhbhum craton (modified after Mukhopadhyay, 2001).

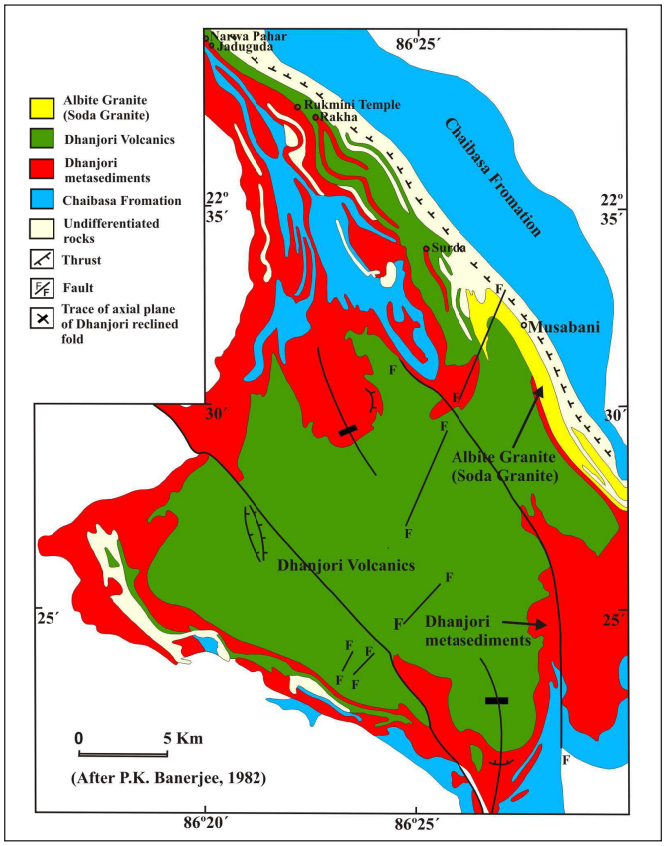

Fig.2. Simplified geological map of the Dhanjori Group showing studied locations around Rakha, Rukmini Temple and Surda (after P.K. Banerjee, 1982).

from the scattered outcrops near Rukmini temple, Surda and Rakha localities, Singhbhum craton, Jharkhand, eastern India. Out of 25 quartzite samples, 10 least altered or fresh samples were selected for thin-sections and whole-rock geochemical analysis. The bulk samples were broken and pulverized to -200 mesh dimensions using a ball mill at the Department of Geology, Aligarh Muslim University (AMU), Aligarh. A whole-rock major elemental and trace elemental (including rare earth elements) analysis was performed by X-ray fluorescence (XRF) spectrometer and inductively coupled plasma mass spectrometer (ICP-MS) techniques respectively at the National Geophysical Research Institute (NGRI), Hyderabad, India. The analytical protocols for data precision and accuracy are given by Krishna et al. (2007) and Satyanarayanan et al. (2018) for XRF and ICP-MS, respectively. The solution was prepared by following the closed digestion method. 50 mg rock sample powder was dissolved in savillex vessels (closed digestion vessel) containing 10 ml acid mixture of HF: HNO_3 in a 7:3 ratio and these vessels were kept on a hot plate at 150°C for 48 hours in closed condition. After complete digestion, 2–3 drops of perchloric acid ($HClO_4$) was added and the entire mixture was evaporated to complete dryness until a crystalline paste was obtained. 10 ml of 1:1 HNO_3 was added to each vessel and these vessels were put on hot plates at ~80°C for 10–15 minutes. After addition of 5 ml of 1 ppm rhodium solution as an internal standard, the volume was diluted to 250 ml with double distilled water. 5 ml of this solution was further diluted to 50 ml for the preparation of the final solution. This solution was used for the estimation of trace (including REEs) elements using ICP-MS techniques. All the available data was standardized against the international reference rock standard GSR4 and JG2. The recovery values of the analytes are listed in Table 5. The analytical precision for major oxides is (<4%) RSD and for trace elements and REEs, it is <5%.

PETROGRAPHY

The studied Dhanjori quartzites possess quartz as the predominant phase, which occurs as common quartz (monocrystalline quartz) with undulose extinction and polycrystalline quartz (recrystallized and stretched quartz, Fig.3a). In addition to quartz, some thin.-sections also contain K-feldspar (microcline, Fig.3c) and plagioclase grains. Plagioclases are often altered to micaceous minerals (sericite, Fig.3b). Mica occurs as muscovite and biotite (Fig.3d). The rock fragment and heavy mineral (zircon) are also present. Monocrystalline quartz has the inclusion of zircon (Fig.3e). The primary cementing material is found to be iron and silica. The modal mineralogy of the studied quartzite samples have been determined by the point-counting method. It is observed that monocrystalline quartz (Qm) ranges from 77.8 to 94.56% (average 87.6%) and polycrystalline quartz (Qp) ranges from 1.3 to 17.9% (average 8.4%), feldspar is around 1 %, and lithic fragment ranges from 1 to 2%. Mica "occurs as lath shaped or a tiny to large elongated flakes" with its abundance ranging from 1.0 to 5.0%. On the ternary diagrams of Dickinson (1985) like Qt-F-L and Qm-F-Lt, the studied samples plot in the craton interior and quartzose field (Figs. 4a and b).

RESULTS

Major Element Geochemistry

Geochemical data (including major and trace elements) of the Dhanjori quartzites are given in Table 1 and 2. Major oxide variations are as SiO_2 (90.60 – 97.84%; average 94.99 %), Al_2O_3 (0.12 – 4.56%; average 1.67 %), Fe_2O_3 (0.13 – 2.74%; average 0.76%), K_2O (0.08–1.28%; average 0.45%), MgO (0.01–0.34%; average 0.15%) and Na_2O (0.02–0.12%; average 0.05%); CaO, MnO, TiO_2 and P_2O_5 are in minor amounts. In the Herron's geochemical plot (1988), the studied samples fall in quartz-arenite and sub-arkose fields (Fig.5a). Whereas in the Na_2O vs. K_2O diagram (Crook, 1974) most of the samples plot in quartz-rich field (Fig.5b). The high value of Al_2O_3 in a few samples is due to the presence of clay minerals and feldspars. K_2O is mainly derived from the weathering of potash feldspar and mica. A low Al_2O_3/SiO_2 (0.001-0.050) ratio indicates quartz enrichment in the sediments whereas, low Na_2O/ K_2O (0.05-0.66) ratio indicates the dominance of K-feldspars over plagioclase in the samples or presence of the micaceous minerals. The K_2O/Al_2O_3 values are applied to point out the primary compositions of sediments (Cox et. al., 1995). For example, K_2O/Al_2O_3 values in feldspars and clay minerals from (0.3 – 0.9) and (0.0 – 0.3) respectively. In the case of studied Dhanjori quartzites, K_2O/Al_2O_3 values vary from 0.13 to 0.82 (average 0.34), which indicates a prevalence of K-feldspars and micas over clay minerals in the provenance. Pearson correlation coefficient (r) values are given in

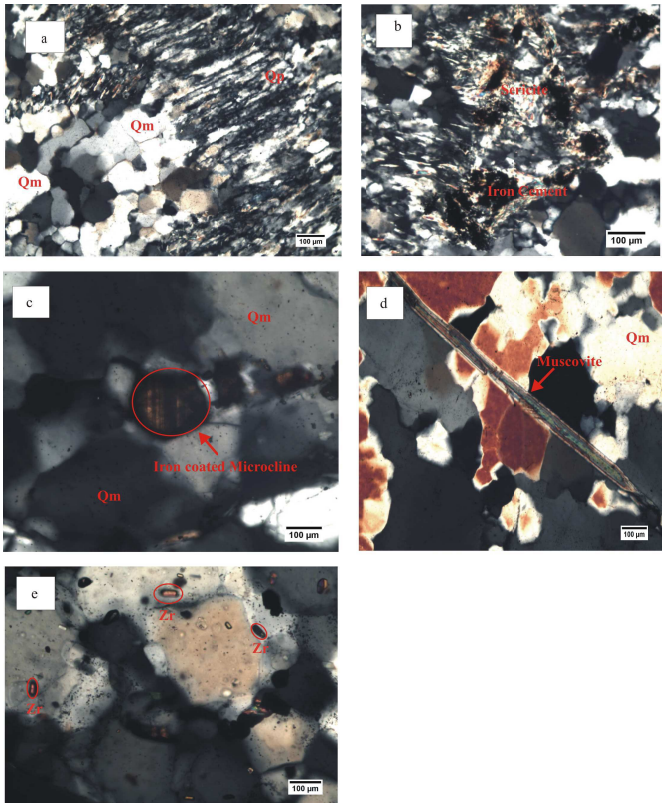

Fig.3. Microphotograph (under crossed-polarized light) of Dhanjori Quartzite showing; **(a)** domination of monocrystalline quartz (Qm) and polycrystalline quartz(Qp); **(b)** Plagioclase altered into sericite and coated iron cement; **(c)** K-feldspar (microcline) coated by iron and surrounded by monocrystalline quartz (Qm); **(d)** Oriented mica (muscovite) embedded in monocrystalline quartz (Qm); **(e)** Monocrystalline quartz exhibiting inclusion of zircon (Zr).

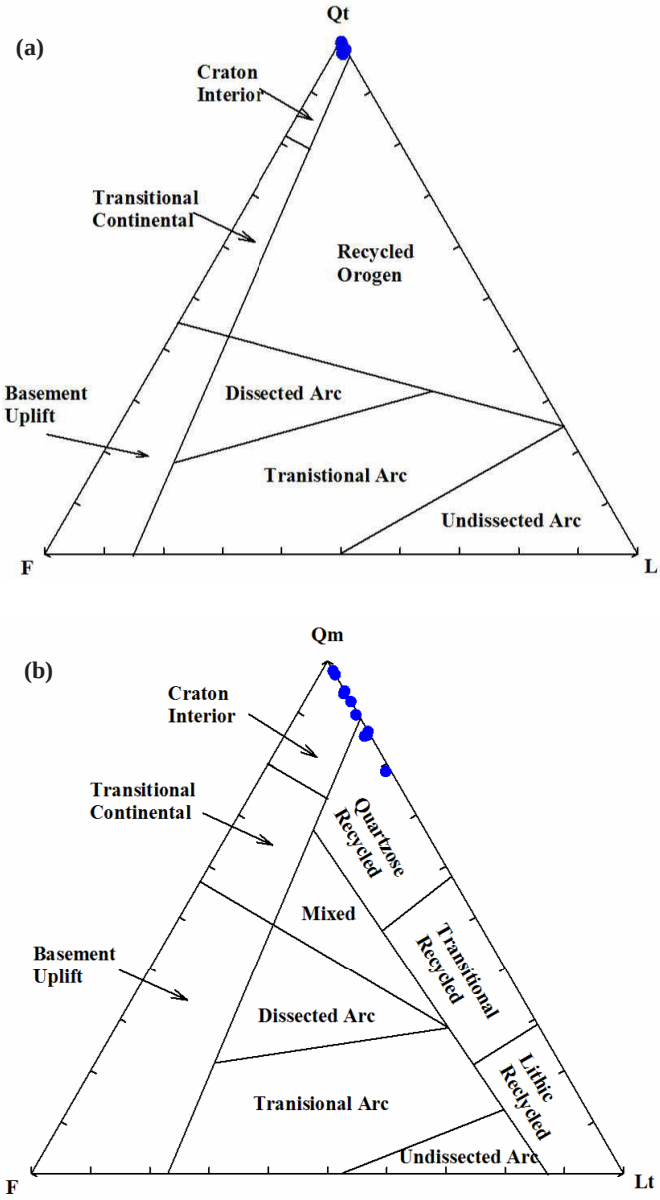

Fig.4. (a) Qt–F–L diagram (Dickinson, 1985); **(b)** Qm-F-Lt diagram (Dickinson, 1985) for the , where, Qt= Total Quartz (Qm+Qp), Qm= monocrystalline Quartz, Qp= Polycrystalline quartz, F= Total Feldspar, L=Total Lithic Fragments, Lt= (L+Qp).

Table 1. Major oxides compositions (wt. %) of Dhanjori quartzite.

Sample No	U-1/RT	U-2/RT	U-4/RT	U-7/RT	U-8/RT	U-9/RT	SU-6	SU-7	U-16/R	U-19/R
SiO_2	94.37	95.83	96.63	95.78	96.41	93.33	95.76	97.84	93.38	90.60
Al_2O_3	2.35	1.95	1.17	0.91	1.18	3.12	0.97	0.12	0.35	4.56
Fe_2O_3	0.35	0.16	0.35	1.09	0.13	0.43	0.82	0.43	2.74	1.14
MnO	0.00	0.00	0.00	0.02	0.00	0.01	0.00	0.00	0.00	0.01
MgO	0.11	0.03	0.01	0.32	0.08	0.28	0.19	0.06	0.04	0.34
CaO	0.01	0.01	0.01	0.01	0.01	0.01	0.01	0.01	0.01	0.01
Na_2O	0.04	0.04	0.03	0.02	0.06	0.07	0.07	0.05	0.04	0.12
K_2O	0.78	0.25	0.19	0.22	0.40	0.85	0.19	0.08	0.28	1.28
TiO_2	0.09	0.03	0.03	0.07	0.06	0.13	0.03	0.02	1.25	0.23
P_2O_5	0.01	0.01	0.01	0.02	0.01	0.01	0.01	0.01	0.01	0.02
Total	98.11	98.31	98.41	98.45	98.32	98.24	98.05	98.61	98.10	98.31
CIA	71.73	84.78	81.78	76.00	68.29	74.41	74.34	41.44	47.47	73.86
CIW	96.67	96.09	95.23	94.36	91.09	95.54	88.35	57.38	81.90	95.28
PIA	94.90	95.49	94.29	92.57	86.62	93.77	85.64	30.73	34.12	93.35
Al_2O_3/SiO_2	0.02	0.02	0.01	0.01	0.01	0.03	0.01	0.00	0.00	0.05
K_2O/Na_2O	20.47	6.92	6.20	9.77	6.51	11.53	2.64	1.52	7.28	10.49
Na_2O/K_2O	0.05	0.14	0.16	0.10	0.15	0.09	0.38	0.66	0.14	0.10
K_2O/Al_2O_3	0.33	0.13	0.16	0.24	0.34	0.27	0.20	0.62	0.82	0.28
Al_2O_3/TiO_2	25.51	64.90	38.93	13.60	18.95	23.96	31.19	6.47	0.28	20.28

Table 2. Trace and rare earth element data in ppm for Dhanjori quartzite

Sample No	U-1/RT	U-2/RT	U-4/RT	U-7/RT	U-8/RT	U-9/RT	SU-6	SU-7	U-16/R	U-19/R
Sc	1.31	0.63	0.95	1.42	1.18	1.60	0.90	0.58	10.62	4.73
V	20.94	3.84	4.84	27.92	3.83	7.33	3.63	3.66	16.21	34.32
Cr	147.26	61.24	49.06	44.27	27.63	83.77	8.75	12.03	23.77	181.63
Co	42.66	97.93	180.07	53.73	102.03	24.64	141.62	104.42	183.97	43.90
Ni	12.65	22.82	28.10	27.12	21.65	9.58	14.63	17.07	27.09	52.36
Cu	24.83	9.90	12.22	20.28	10.33	9.59	18.44	16.53	14.60	71.18
Zn	1.97	1.44	5.84	3.19	2.22	1.51	1.92	10.65	3.58	2.34
Ga	1.78	0.96	1.08	1.55	1.20	1.67	1.31	0.79	1.55	4.39
Rb	23.06	10.46	8.51	10.10	12.19	14.10	6.02	3.93	11.81	43.65
Sr	3.25	4.51	6.12	4.73	4.23	4.70	4.28	5.34	6.40	8.66
Y	5.84	1.63	4.95	3.94	2.33	7.23	1.08	0.87	14.08	13.13
Zr	165.36	16.81	37.31	38.92	8.05	458.48	5.75	2.55	588.96	130.94
Nb	3.05	1.71	3.15	1.83	1.11	3.27	0.79	4.13	29.48	3.11
Cs	0.71	0.30	0.28	0.33	0.40	0.17	0.26	0.27	0.23	1.12
Ba	88.32	42.22	62.28	44.60	48.94	64.08	21.99	18.15	40.30	123.90
Hf	4.63	0.54	1.35	1.09	0.27	13.28	0.20	0.07	18.96	3.84
Ta	3.37	1.84	3.17	2.89	1.20	1.15	3.17	14.84	4.54	2.99
Pb	4.29	4.11	12.09	10.01	7.10	7.36	4.78	4.44	11.42	8.48
Th	0.90	0.09	0.93	0.58	0.21	2.24	0.10	0.12	17.38	1.84
U	0.71	0.36	1.28	2.13	0.59	0.90	0.66	0.66	4.38	1.51
La	14.16	4.32	4.39	4.14	6.17	3.91	3.59	2.00	4.25	16.51
Ce	6.49	3.56	7.06	5.44	11.88	7.83	10.60	6.43	7.83	26.89
Pr	3.15	0.60	0.77	1.02	1.34	0.91	0.86	0.47	0.98	4.45
Nd	11.08	1.93	2.85	3.75	4.74	3.28	3.04	1.72	3.67	16.18
Sm	1.77	0.44	0.63	0.78	0.83	0.66	0.54	0.32	0.84	3.35
Eu	0.36	0.08	0.13	0.21	0.18	0.14	0.10	0.06	0.28	0.55
Gd	1.40	0.36	0.65	0.70	0.66	0.74	0.40	0.25	1.28	2.89
Tb	0.23	0.06	0.14	0.13	0.10	0.17	0.06	0.04	0.33	0.51
Dy	1.14	0.35	0.84	0.78	0.51	1.12	0.25	0.19	2.33	2.72
Ho	0.24	0.08	0.19	0.17	0.11	0.28	0.05	0.04	0.58	0.55
Er	0.62	0.21	0.54	0.46	0.28	0.90	0.11	0.09	1.85	1.41
Tm	0.10	0.04	0.09	0.07	0.05	0.16	0.01	0.01	0.34	0.21
Yb	0.75	0.31	0.71	0.55	0.37	1.32	0.10	0.09	2.99	1.63
Lu	0.13	0.06	0.12	0.09	0.06	0.23	0.02	0.01	0.54	0.27
ΣREE	41.62	12.38	19.10	18.30	27.27	21.62	19.72	11.71	28.10	78.12
Zr/Sc	126.00	26.76	39.15	27.47	6.84	287.04	6.39	4.36	55.45	27.68
Th/Sc	0.68	0.15	0.98	0.41	0.18	1.40	0.11	0.21	1.64	0.39
La/Sc	10.79	6.88	4.61	2.92	5.25	2.45	3.98	3.42	0.40	3.49
Th/Co	0.02	0.00	0.01	0.01	0.00	0.09	0.00	0.00	0.09	0.04
Th/U	1.26	0.26	0.73	0.27	0.36	2.49	0.14	0.19	3.97	1.22
La/Co	0.33	0.04	0.02	0.08	0.06	0.16	0.03	0.02	0.02	0.38
Cr/Th	164.12	666.25	52.64	76.62	129.94	37.44	92.00	97.26	1.37	98.55
Co/Th	0.00	0.00	0.00	0.00	0.00	0.00	0.00	0.00	0.00	0.00
U/Th	0.79	3.89	1.38	3.69	2.79	0.40	6.96	5.33	0.25	0.82
Eu/Eu*	0.69	0.60	0.63	0.87	0.76	0.60	0.63	0.63	0.81	0.55
LREE/HREE	11.95	10.28	6.30	7.12	17.50	4.18	32.20	24.45	2.13	9.69

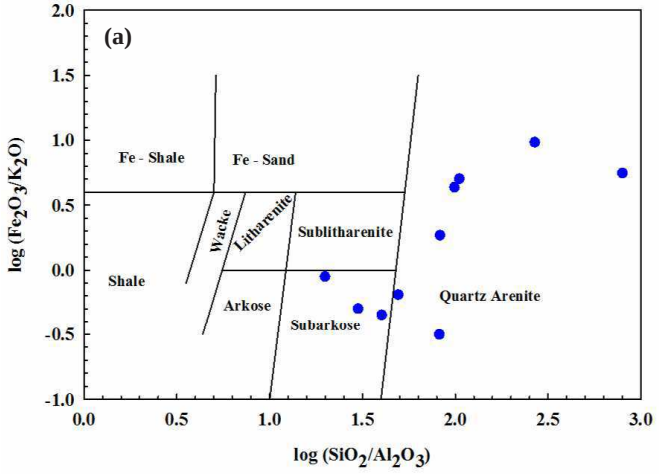

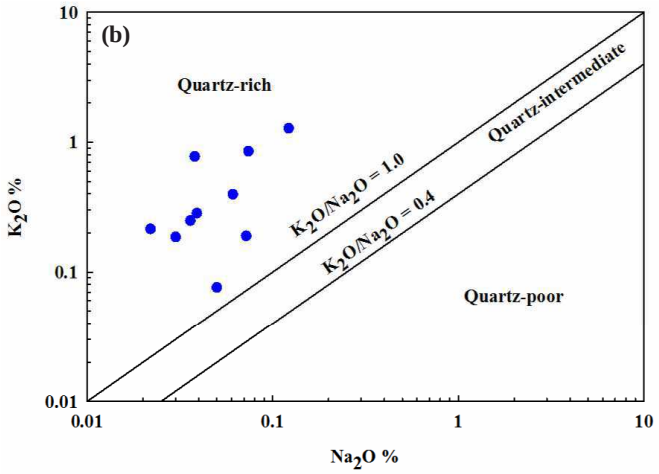

Fig.5. (a) log (SiO_2/Al_2O_3) vs. log (Fe_2O_3/K_2O) diagram by Herron (1988) and **(b)** Na_2O vs. K_2O diagram by Crook (1974) for the classification of studied Dhanjori quartzites.

Table 4. The Al_2O_3 exhibits a negative correlation against SiO_2 [r = –0.785, significance level (P) = 0.007)] as expected because of SiO_2 and Al_2O_3 contents in sedimentary rocks are controlled by quartz and aluminous clay phases respectively. Whereas, positive correlations between Al_2O_3 and K_2O (r = 0.937, P = 0.0001) and Al_2O_3 and Na_2O (r = 0.709, P = 0.022) is due to K-bearing minerals. The low concentrations of CaO (0.01%), Na_2O (0.02 – 0.12%), Al_2O_3 (0.12 – 4.56%) are compatible with the low plagioclase content. The SiO_2/Al_2O_3 is > 10, which suggests highly mature nature of sediments.

Trace and Rare Earth Element Geochemistry

The ranges of some transitional elements in the studied samples are Sc (0.58-10.62, average 2.39), Cr (8.75-181.63, average 63.94), Ni (9.58-52.36, average 23.31), and V (3.66-34.32, average 12.65). In addition to these trace elements, REEs show negative correlation against SiO_2 (Table 4) which indicates a decrease in elemental abundance with quartz dilution. Al_2O_3 is positively correlated with K_2O (r = 0.937, P = 0.0001), Rb (r = 0.864, P = 0.001), Ba (r = 0.875, P = 0.001), and Cs (r = 0.719, P = 0.019) suggesting that these elements are fixed in K-rich clays. Rb and Ba show a strong correlation against K_2O (r = 0.919, P = 0.0002 and r = 0.905, P = 0.0003 respectively), indicating that K-feldspars and clay minerals (i.e. kaolinite or illite) host these elements (Újvári et al., 2008). The positive relationship of Al_2O_3 with Cr (r = 0.893, P = 0.001) and V (r = 0.499, P = 0.142) suggests that these elements are controlled by alumina-silicate phases.

Table 3. Range of elemental ratios of Dhanjori quartzite compared with the ratios derived from felsic rocks, mafic rocks and upper continental crust.

Elemental ratio	Dhanjori quartzite	Ranges in sediments from felsic sources [1]	Ranges in sediments from mafic sources [1]	Upper Continental Crust [2]
Eu/Eu*	0.55-0.87	0.40-0.94	0.71-0.95	0.63
La/Sc	0.40-10.79	2.50-16.3	0.43-0.86	2.21
Th/Sc	0.11-1.40	0.84-20.5	0.05-0.22	0.79
La/Co	0.02-0.38	1.80-13.8	0.14-0.38	1.76
Th/Co	0.0006-0.09	0.67-19.4	0.04-1.40	0.63
Cr/Th	1.37-666.25	4.00-15.0	25-500	7.76

[1]Cullers et al (1988); Cullers (2000); Cullers and Podkovyrov (2000).
[2]McLennan (2001); Taylor and McLennan (1985).

A few large ion lithophile elements (LILEs) such as Rb (3.93–43.65, average 14.38), Sr (3.25–8.66, average 5.22), Ba (18.15–123.90, average 55.48), Th (0.09–17.38, average 2.44), and U (0.36– 4.38, average 1.32) show variations. Such a high Rb contents in the studied samples reflect the presence of high proportion of K-feldspar in the rocks of provenance. Upper continental crust (UCC) normalized multi-element spider diagram of trace elements (Fig.6) shows enhancement of Zr, Rb, U, Y, and Hf and reduction of K, Th, Nb, and Sr. The depletion of Sr suggests a minor enrichment of plagioclase, this is further verified by negative Eu-anomaly of studied samples. Zr enrichment is attributed to the abundance of zircon mineral, which implies the dominance of silicic rocks in the source terrain. The chondrite normalized REE diagram (Fig.7) show slight enrichment of light-REE (LREE) with negative Ce anomaly, which indicates oxidizing environment (La_N/Sm_N= 3.11 to 6.19; average 4.17) and flat heavy-REE (HREE) (Gd_N/Yb_N = 0.35 to 3.12; average 1.34) pattern with negative Eu anomaly (0.55 to 0.87; average 0.68). A high LREE and a low HREE may be attributed to the quartz dilution. The effect is further accompanied by low ΣREE ranging from 11.71 – 78.12 ppm (average 27.29) and is lower than the average UCC (Taylor and McLennan, 1985).

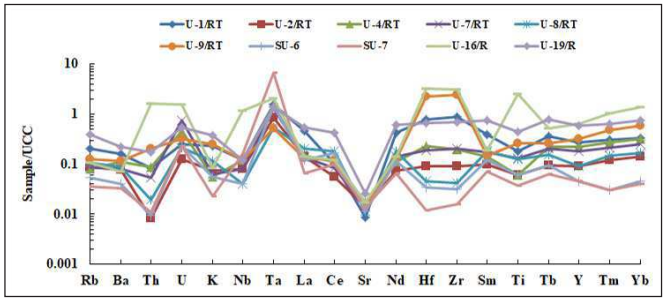

Fig.6. Upper continental crust trace element normalized plot for the studied Dhanjori quartzites (Taylor and McLennan, 1985).

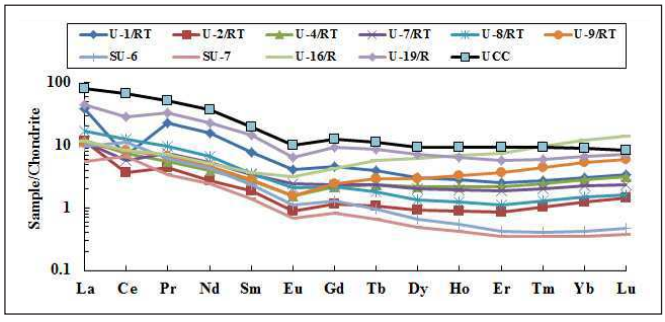

Fig.7. Chondrite normalized (Taylor and McLennan, 1985) rare earth element (REE) pattern for the studied Dhanjori quartzites.

Table 4. Correlation coefficient (r) and significance level (P) of the Dhanjori quartzite (number of sample, n = 10).

	SiO_2	Al_2O_3	Fe_2O_3	MnO	MgO	CaO	Na_2O	K_2O	TiO_2	P_2O_5	Sc	V	Cr	Co	Ni	Cu	Zn	Ga	Rb	Sr	Y	Zr
SiO_2	1.000																					
Al_2O_3	-0.785	1.000																				
	0.007																					
Fe_2O_3	-0.459	-0.177	1.000																			
	0.182	**0.625**																				
MnO	-0.102	0.057	0.133	1.000																		
	0.779	**0.876**	**0.713**																			
MgO	-0.572	0.592	0.093	0.711	1.000																	
	0.083	**0.071**	**0.798**	**0.021**																		
CaO	-0.730	0.855	-0.055	0.376	0.640	1.000																
	0.016	**0.001**	**0.881**	**0.284**	**0.046**																	
Na_2O	-0.655	0.709	0.021	-0.164	0.549	0.453	1.000															
	0.040	**0.022**	**0.954**	**0.651**	**0.100**	**0.189**																
K_2O	-0.866	0.937	0.005	0.059	0.596	0.810	0.733	1.000														
	0.001	**0.0001**	**0.989**	**0.872**	**0.0690**	**0.005**	**0.016**															
TiO_2	-0.420	-0.191	0.915	-0.131	-0.181	-0.056	-0.056	0.009	1.000													
	0.227	**0.596**	**0.0002**	**0.718**	**0.616**	**0.878**	**0.878**	**0.980**														
P_2O_5	-0.773	0.556	0.527	0.369	0.553	0.569	0.389	0.571	0.333	1.000												
	0.009	**0.095**	**0.117**	**0.294**	**0.097**	**0.086**	**0.266**	**0.085**	**0.347**													
Sc	-0.578	-0.015	0.932	-0.095	-0.031	0.071	0.128	0.182	0.971	0.518	1.000											
	0.080	**0.967**	**0.0001**	**0.794**	**0.932**	**0.846**	**0.724**	**0.615**	**0.0000**	**0.126**												
V	-0.691	0.499	0.435	0.568	0.645	0.575	0.279	0.605	0.229	0.895	0.394	1.000										
	0.027	**0.142**	**0.209**	**0.087**	**0.044**	**0.082**	**0.436**	**0.063**	**0.524**	**0.0005**	**0.260**											
Cr	-0.745	0.893	-0.091	0.080	0.456	0.764	0.497	0.905	-0.103	0.633	0.064	0.683	1.000									
	0.013	**0.001**	**0.803**	**0.826**	**0.185**	**0.0101**	**0.144**	**0.0003**	**0.776**	**0.049**	**0.861**	**0.030**										
Co	0.381	-0.662	0.364	-0.525	-0.697	-0.800	-0.350	-0.660	0.428	-0.238	0.337	-0.462	-0.639	1.000								
	0.278	**0.037**	**0.302**	**0.119**	**0.025**	**0.006**	**0.321**	**0.038**	**0.218**	**0.509**	**0.341**	**0.178**	**0.047**									
Ni	-0.527	0.426	0.347	0.076	0.294	0.323	0.450	0.403	0.205	0.836	0.405	0.641	0.446	0.024	1.000							
	0.116	**0.220**	**0.326**	**0.834**	**0.410**	**0.362**	**0.192**	**0.248**	**0.570**	**0.003**	**0.245**	**0.046**	**0.196**	**0.947**								
Cu	-0.711	0.690	0.206	0.115	0.571	0.495	0.728	0.730	0.018	0.817	0.246	0.772	0.747	-0.371	0.788	1.000						
	0.021	**0.027**	**0.567**	**0.752**	**0.084**	**0.146**	**0.017**	**0.017**	**0.961**	**0.004**	**0.493**	**0.009**	**0.013**	**0.291**	**0.007**							
Zn	0.529	-0.523	-0.026	-0.187	-0.379	-0.591	-0.226	-0.463	-0.052	-0.285	-0.091	-0.239	-0.381	0.326	-0.024	-0.114	1.000					
	0.116	**0.121**	**0.944**	**0.605**	**0.280**	**0.072**	**0.530**	**0.178**	**0.887**	**0.425**	**0.803**	**0.506**	**0.277**	**0.357**	**0.948**	**0.754**						
Ga	-0.875	0.809	0.271	0.155	0.658	0.657	0.775	0.863	0.129	0.845	0.353	0.791	0.803	-0.437	0.754	0.950	-0.319	1.000				
	0.001	**0.005**	**0.449**	**0.670**	**0.039**	**0.039**	**0.009**	**0.001**	**0.722**	**0.002**	**0.317**	**0.007**	**0.005**	**0.206**	**0.012**	**0.0000**	**0.368**					
Rb	-0.850	0.864	0.127	0.051	0.517	0.720	0.691	0.919	0.076	0.772	0.283	0.758	0.918	-0.506	0.680	0.899	-0.374	0.953	1.000			
	0.002	**0.001**	**0.726**	**0.889**	**0.125**	**0.019**	**0.029**	**0.0002**	**0.835**	**0.009**	**0.428**	**0.011**	**0.0002**	**0.135**	**0.031**	**0.0004**	**0.287**	**0.0000**				
Sr	-0.563	0.375	0.471	-0.101	0.241	0.209	0.545	0.389	0.365	0.709	0.540	0.463	0.329	0.146	0.872	0.700	0.192	0.695	0.565	1.000		
	0.090	**0.286**	**0.170**	**0.782**	**0.503**	**0.561**	**0.103**	**0.266**	**0.300**	**0.022**	**0.107**	**0.178**	**0.353**	**0.687**	**0.001**	**0.024**	**0.595**	**0.026**	**0.089**			
Y	-0.855	0.441	0.732	0.002	0.264	0.425	0.372	0.604	0.746	0.726	0.856	0.637	0.508	-0.013	0.565	0.539	-0.222	0.689	0.652	0.684	1.000	
	0.002	**0.203**	**0.016**	**0.995**	**0.462**	**0.221**	**0.290**	**0.065**	**0.013**	**0.017**	**0.002**	**0.048**	**0.134**	**0.971**	**0.088**	**0.108**	**0.537**	**0.028**	**0.041**	**0.029**		
Zr	-0.572	0.126	0.663	-0.026	0.072	0.263	0.067	0.305	0.796	0.204	0.758	0.179	0.114	0.029	-0.078	-0.062	-0.221	0.164	0.142	0.198	0.746	1.000
	0.084	**0.728**	**0.037**	**0.944**	**0.843**	**0.462**	**0.854**	**0.391**	**0.006**	**0.572**	**0.011**	**0.621**	**0.753**	**0.936**	**0.830**	**0.865**	**0.540**	**0.650**	**0.695**	**0.583**	**0.013**	
Nb	-0.287	-0.312	0.880	-0.181	-0.303	-0.175	-0.173	-0.114	0.984	0.223	0.927	0.128	-0.196	0.502	0.119	-0.090	0.088	-0.005	-0.050	0.314	0.666	0.772
	0.422	**0.380**	**0.0008**	**0.617**	**0.395**	**0.629**	**0.633**	**0.753**	**0.0000**	**0.535**	**0.0001**	**0.724**	**0.587**	**0.139**	**0.744**	**0.806**	**0.809**	**0.990**	**0.891**	**0.377**	**0.035**	**0.009**
Cs	-0.637	0.719	0.004	0.019	0.408	0.530	0.605	0.772	-0.084	0.693	0.121	0.730	0.858	-0.451	0.671	0.917	-0.221	0.869	0.935	0.471	0.442	-0.147

Table 4. Contd....

	SiO_2	Al_2O_3	Fe_2O_3	MnO	MgO	CaO	Na_2O	K_2O	TiO_2	P_2O_5	Sc	V	Cr	Co	Ni	Cu	Zn	Ga	Rb	Sr	Y	Zr
	0.048	**0.019**	**0.990**	**0.959**	**0.241**	**0.115**	**0.064**	**0.009**	**0.818**	**0.026**	**0.738**	**0.017**	**0.002**	**0.191**	**0.034**	**0.0002**	**0.539**	**0.001**	**0.0001**	**0.170**	**0.201**	**0.686**
Ba	-0.771	0.875	-0.019	0.044	0.440	0.704	0.532	0.905	-0.023	0.670	0.160	0.688	0.952	-0.501	0.581	0.761	-0.380	0.848	0.939	0.468	0.610	0.146
	0.009	**0.001**	**0.958**	**0.905**	**0.203**	**0.023**	**0.114**	**0.0003**	**0.949**	**0.034**	**0.658**	**0.028**	**0.0000**	**0.140**	**0.078**	**0.011**	**0.278**	**0.002**	**0.0001**	**0.172**	**0.061**	**0.688**
Hf	-0.555	0.085	0.698	-0.045	0.035	0.222	0.046	0.266	0.832	0.209	0.791	0.171	0.080	0.086	-0.057	-0.070	-0.201	0.149	0.122	0.217	0.753	0.998
	0.096	**0.815**	**0.025**	**0.901**	**0.924**	**0.537**	**0.900**	**0.457**	**0.003**	**0.562**	**0.006**	**0.637**	**0.827**	**0.813**	**0.875**	**0.847**	**0.578**	**0.681**	**0.736**	**0.547**	**0.012**	**0.0000**
Ta	0.412	-0.458	0.045	-0.173	-0.287	-0.484	-0.101	-0.363	0.002	-0.239	-0.034	-0.162	-0.300	0.170	-0.102	-0.013	0.915	-0.237	-0.286	0.112	-0.207	-0.162
	0.237	**0.183**	**0.902**	**0.633**	**0.422**	**0.156**	**0.781**	**0.302**	**0.996**	**0.506**	**0.925**	**0.655**	**0.400**	**0.639**	**0.779**	**0.972**	**0.0002**	**0.510**	**0.423**	**0.758**	**0.565**	**0.655**
Pb	-0.230	-0.081	0.543	0.202	0.068	-0.066	-0.139	-0.018	0.491	0.404	0.530	0.310	-0.061	0.384	0.474	0.067	0.054	0.181	0.070	0.538	0.571	0.380
	0.523	**0.823**	**0.105**	**0.575**	**0.851**	**0.856**	**0.701**	**0.961**	**0.150**	**0.247**	**0.115**	**0.383**	**0.866**	**0.273**	**0.166**	**0.853**	**0.883**	**0.618**	**0.847**	**0.109**	**0.085**	**0.279**
Th	-0.376	-0.230	0.899	-0.142	-0.217	-0.094	-0.110	-0.036	0.995	0.275	0.950	0.172	-0.147	0.458	0.145	-0.055	-0.026	0.063	0.010	0.332	0.721	0.818
	0.285	**0.522**	**0.0004**	**0.696**	**0.547**	**0.797**	**0.763**	**0.922**	**0.0000**	**0.441**	**0.0000**	**0.635**	**0.686**	**0.183**	**0.689**	**0.880**	**0.944**	**0.863**	**0.978**	**0.349**	**0.017**	**0.004**
U	-0.368	-0.240	0.951	0.183	0.001	-0.067	-0.168	-0.059	0.913	0.479	0.908	0.417	-0.120	0.393	0.336	0.077	0.022	0.167	0.058	0.439	0.732	0.682
	0.295	**0.504**	**0.0000**	**0.613**	**0.998**	**0.854**	**0.643**	**0.871**	**0.0002**	**0.161**	**.0003**	**0.231**	**0.742**	**0.261**	**0.342**	**0.832**	**0.951**	**0.644**	**0.875**	**0.205**	**0.016**	**0.030**
La	-0.688	0.749	0.0002	-0.018	0.354	0.570	0.518	0.829	-0.022	0.624	0.151	0.704	0.918	-0.476	0.513	0.806	-0.363	0.814	0.929	0.319	0.494	0.006
	0.028	**0.013**	**0.999**	**0.960**	**0.315**	**0.085**	**0.126**	**0.003**	**0.951**	**0.054**	**0.677**	**0.023**	**0.0002**	**0.164**	**0.130**	**0.005**	**0.303**	**0.004**	**0.0001**	**0.369**	**0.146**	**0.988**
Ce	-0.688	0.662	0.170	-0.079	0.516	0.404	0.896	0.718	0.050	0.629	0.272	0.529	0.572	-0.229	0.746	0.886	-0.186	0.899	0.821	0.719	0.521	-0.013
	0.028	**0.037**	**0.638**	**0.829**	**0.127**	**0.247**	**0.0004**	**0.019**	**0.890**	**0.052**	**0.447**	**0.116**	**0.084**	**0.524**	**0.013**	**0.0006**	**0.606**	**0.0004**	**0.004**	**0.019**	**0.123**	**0.972**
Pr	-0.740	0.762	0.076	0.040	0.460	0.580	0.615	0.857	0.009	0.685	0.203	0.758	0.901	-0.491	0.579	0.882	-0.322	0.889	0.959	0.419	0.546	0.032
	0.014	**0.011**	**0.835**	**0.914**	**0.181**	**0.079**	**0.059**	**0.002**	**0.979**	**0.029**	**0.575**	**0.011**	**0.0004**	**0.150**	**0.080**	**0.0007**	**0.364**	**0.0006**	**0.0000**	**0.229**	**0.102**	**0.930**
Nd	-0.749	0.759	0.096	0.045	0.469	0.576	0.622	0.857	0.024	0.699	0.220	0.768	0.897	-0.481	0.596	0.891	-0.311	0.899	0.962	0.443	0.564	0.042
	0.013	**0.011**	**0.792**	**0.901**	**0.172**	**0.081**	**0.055**	**0.002**	**0.947**	**0.025**	**0.541**	**0.009**	**0.0004**	**0.160**	**0.069**	**0.0005**	**0.381**	**0.0004**	**0.0000**	**0.200**	**0.090**	**0.908**
Sm	-0.798	0.778	0.171	0.059	0.504	0.600	0.672	0.858	0.079	0.784	0.291	0.794	0.878	-0.435	0.710	0.939	-0.290	0.954	0.982	0.581	0.632	0.071
	0.006	**0.008**	**0.637**	**0.871**	**0.137**	**0.067**	**0.034**	**0.002**	**0.829**	**0.007**	**0.414**	**0.006**	**0.0008**	**0.209**	**0.021**	**0.0001**	**0.416**	**0.0000**	**0.0000**	**0.078**	**0.050**	**0.845**
Eu	-0.823	0.657	0.370	0.134	0.457	0.562	0.522	0.799	0.295	0.821	0.481	0.867	0.816	-0.357	0.686	0.858	-0.317	0.904	0.934	0.551	0.758	0.244
	0.003	**0.039**	**0.293**	**0.712**	**0.184**	**0.091**	**0.122**	**0.006**	**0.407**	**0.004**	**0.160**	**0.001**	**0.004**	**0.311**	**0.028**	**0.002**	**0.372**	**0.0003**	**0.0001**	**0.099**	**0.011**	**0.496**
Gd	-0.878	0.726	0.375	0.043	0.465	0.583	0.636	0.838	0.304	0.841	0.504	0.812	0.823	-0.321	0.744	0.899	-0.282	0.953	0.959	0.680	0.803	0.281
	0.0008	**0.018**	**0.286**	**0.906**	**0.176**	**0.077**	**0.048**	**0.003**	**0.393**	**0.002**	**0.137**	**0.004**	**0.003**	**0.366**	**0.014**	**0.0004**	**0.431**	**0.0000**	**0.0000**	**0.031**	**0.005**	**0.432**
Tb	-0.908	0.632	0.555	0.031	0.400	0.539	0.552	0.769	0.513	0.845	0.686	0.783	0.721	-0.193	0.723	0.796	-0.264	0.890	0.874	0.729	0.928	0.484
	0.0003	**0.050**	**0.096**	**0.933**	**0.253**	**0.108**	**0.098**	**0.009**	**0.130**	**0.002**	**0.029**	**0.007**	**0.018**	**0.592**	**0.018**	**0.006**	**0.461**	**0.0006**	**0.0009**	**0.017**	**0.0001**	**0.157**
Dy	-0.891	0.528	0.675	0.024	0.333	0.483	0.463	0.679	0.658	0.807	0.801	0.722	0.604	-0.088	0.669	0.675	-0.241	0.797	0.765	0.731	0.983	0.627
	0.001	**0.117**	**0.032**	**0.948**	**0.346**	**0.157**	**0.177**	**0.031**	**0.039**	**0.005**	**0.005**	**0.018**	**0.064**	**0.809**	**0.035**	**0.032**	**0.503**	**0.006**	**0.010**	**0.016**	**0.0000**	**0.052**
Ho	-0.859	0.440	0.741	0.008	0.268	0.432	0.382	0.604	0.751	0.743	0.864	0.651	0.508	-0.016	0.586	0.556	-0.231	0.701	0.664	0.690	0.999	0.730
	0.002	**0.203**	**0.014**	**0.982**	**0.453**	**0.212**	**0.276**	**0.064**	**0.012**	**0.014**	**0.001**	**0.042**	**0.134**	**0.964**	**0.075**	**0.095**	**0.521**	**0.024**	**0.036**	**0.027**	**0.0000**	**0.016**
Er	-0.806	0.343	0.787	-0.007	0.198	0.373	0.293	0.516	0.824	0.662	0.906	0.566	0.402	0.054	0.492	0.427	-0.216	0.590	0.550	0.633	0.990	0.814
	0.005	**0.331**	**0.007**	**0.984**	**0.583**	**0.289**	**0.411**	**0.127**	**0.003**	**0.037**	**0.0003**	**0.088**	**0.249**	**0.883**	**0.149**	**0.218**	**0.549**	**0.072**	**0.099**	**0.050**	**0.0000**	**0.004**
Tm	-0.749	0.253	0.817	-0.032	0.126	0.310	0.220	0.431	0.876	0.591	0.932	0.490	0.308	0.121	0.419	0.323	-0.200	0.494	0.453	0.580	0.966	0.858
	0.013	**0.480**	**0.004**	**0.931**	**0.728**	**0.383**	**0.542**	**0.214**	**0.001**	**0.072**	**0.0001**	**0.151**	**0.387**	**0.739**	**0.229**	**0.362**	**0.580**	**0.146**	**0.189**	**0.079**	**0.0000**	**0.002**
Yb	-0.708	0.195	0.831	-0.047	0.080	0.269	0.171	0.374	0.903	0.541	0.942	0.438	0.246	0.163	0.369	0.256	-0.188	0.430	0.388	0.543	0.944	0.879
	0.022	**0.590**	**0.003**	**0.898**	**0.826**	**0.453**	**0.636**	**0.286**	**0.0003**	**0.106**	**0.0000**	**0.206**	**0.494**	**0.653**	**0.294**	**0.476**	**0.602**	**0.215**	**0.268**	**0.105**	**0.0000**	**0.001**
Lu	-0.684	0.162	0.838	-0.064	0.048	0.241	0.146	0.343	0.918	0.514	0.948	0.409	0.215	0.189	0.341	0.222	-0.181	0.395	0.355	0.520	0.930	0.887
	0.029	**0.655**	**0.003**	**0.860**	**0.896**	**0.502**	**0.687**	**0.332**	**0.0002**	**0.129**	**0.0000**	**0.241**	**0.552**	**0.601**	**0.334**	**0.538**	**0.617**	**0.258**	**0.314**	**0.123**	**0.0001**	**0.001**

DISCUSSION

Provenance

Several authors have used geochemistry (including REEs, HFSEs, and TTEs) of sedimentary rocks to know their source character (e.g., Cullers et al., 1988; Taylor and McLennan, 1985; Armstrong-Altrin et al., 2004; Mir et al., 2015). In the discrimination function diagram (after Roser and Korsch, 1988), studied samples of the Dhanjori Group fall in quartzose sedimentary field (Fig.8a). Roser (2000) stated that the recycled material of felsic igneous rocks does not plot in the igneous fields; however, such sediments do plot in the quartzose field. Zr vs. TiO_2 diagram (Hayashi et al. 1997; Fig.8b) shows that the analyzed samples plot in the felsic and mafic fields. According to Hayashi et al. (1997), Al_2O_3/TiO_2 ratio ranges from (3 to 8), (8 to 21) and (21 to 7) in mafic, intermediate, and felsic igneous rocks respectively. In present samples, Al_2O_3/TiO_2 value ranges from 6.47–64.90 (except sample No. U-16/R = 0.28). Hence, high values of Al_2O_3/TiO_2 indicate felsic igneous rocks are the dominated source for Dhanjori quartzite. Al_2O_3/TiO_2 values of studied quartzites are computed in the following equation of Hayashi et al. (1997)

$$SiO_2 \text{ (wt. \%)} = 39.34 + 1.2578\ (Al_2O_3/TiO_2) - 0.0109\ (Al_2O_3/TiO_2)^2.$$

Therefore, the derived SiO_2 contents (39.69 to 75.06, average 60.31 wt. %) from the equation implies felsic igneous rocks as the source of

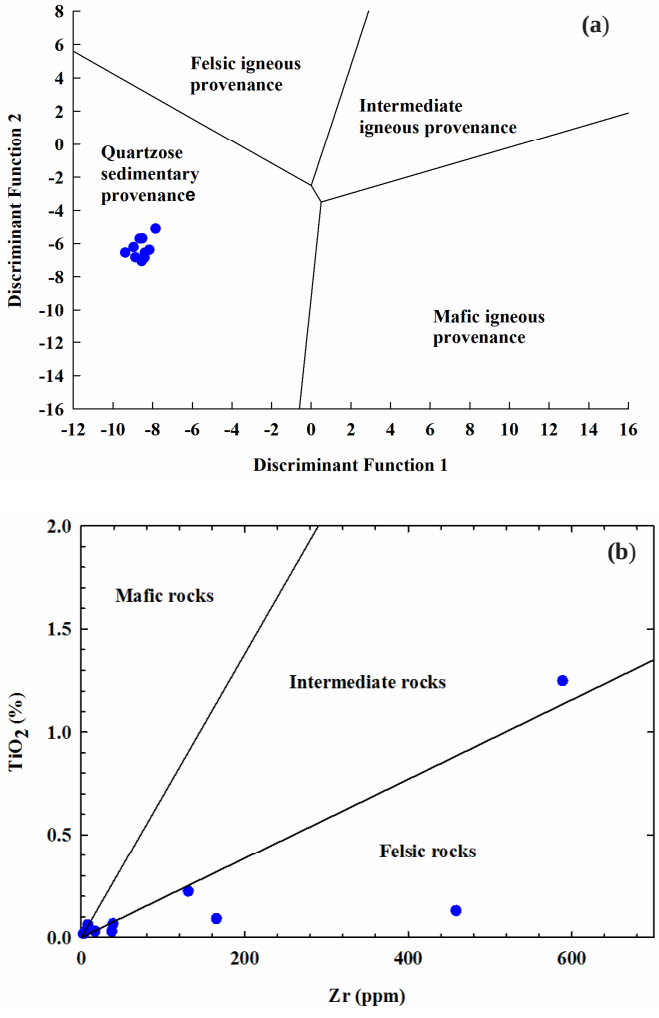

Fig.8. (a) Discriminant function plot (Roser and Korsch, 1988) and **(b)** TiO_2-Zr plot (Hayashi et al., 1997) for the studied Dhanjori quartzites.

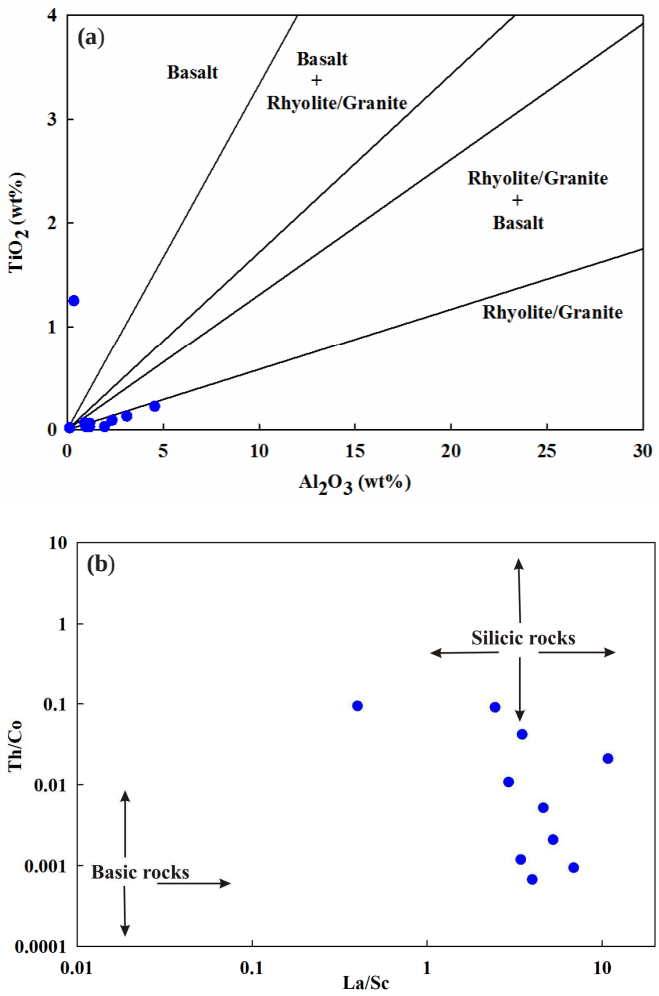

Fig.9. (a) Al_2O_3 vs. TiO_2 diagram (after Ekosse, 2001),and **(b)** La/Sc vs. Th/Co diagram (after Cullers, 2002)for the studied Dhanjori quartzites.

studied quartzites. Al_2O_3 vs. TiO_2 plot had been used by Ekosse (2001) to differentiate between granite and basaltic source rocks; such a plot supports the presence of mixed provenance for the studied Dhanjori quartzite (Fig.9a). Further, La/Sc vs. Th/Co (after Cullers, 2002) plot also supports mixed (felsic plus mafic) provenance (Fig.9b) for the studied samples. Furthermore, some useful trace elemental ratios of analyzed samples indicate that these are felsic, mafic, and upper continental crust derived sediments. Further, ratios like Eu/Eu* (~ 0.68), La/Sc (~ 4.42), Th/Sc (~ 0.61), La/Co (~ 0.11), Th/Co (~ 0.03) and Cr/Th (~ 141.62) also suggest that studied samples have been derived from mixed (felsic plus mafic) source rocks (Table 3).

The triangular diagram of La-Th-Sc (Taylor and McLennan, 1985) is utilized to determine the nature of the source. The average compositions of the granite, TTG, andesite, basalt, komatiite (Condie, 1993), and UCC (Taylor and McLennan, 1985) are used for the assessment of the provenance characteristics of the studied samples. The studied samples when plotted on La-Th-Sc ternary diagram, show close association with TTG, granite, UCC and andesite compositions (Fig.10); such an association implies that the sediments for the studied samples have been derived from the source that had major amounts of felsic and minor amounts of mafic rocks. From the above discussion, it is concluded that mixed (felsic plus mafic) provenance is suggested for the studied samples of the Dhanjori Group. The poorly mixed source is also suggested by earlier workers like De et al. (2015) for the Dhanjori Group. Since the Dhanjori Group is surrounded in the east by the Older Metamorphic Group (OMG) and in the

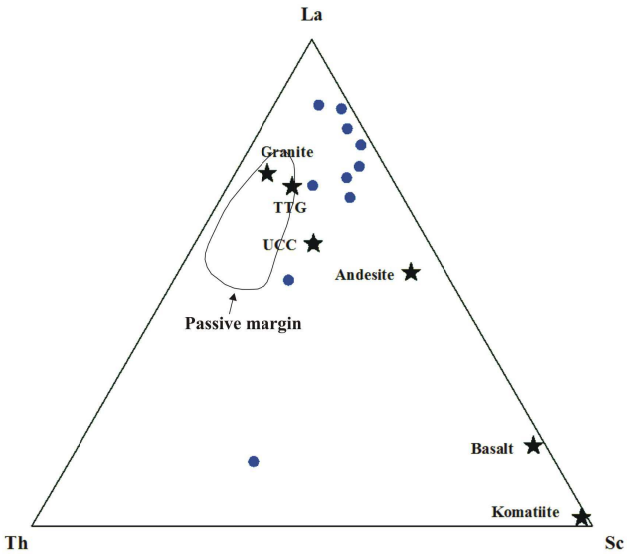

Fig.10. La-Sc-Th plot for the studied Dhanjori quartzites; UCC values are taken from Taylor and McLennan, 1985; Granite, Basalt, Andesite, TTG and Komatiite are after Condie, 1993. Passive margin field (Bhatia and Crook, 1986).

south by the Singhbhum granitoid complex (SBGC), both of them older than the Dhanjori Group. Therefore, it is inferred that the metasediments and ortho-amphibolites of OMG, Singhbhum granitoid complex (SBGC), and associated Archaean metavolcanic suites may have been the probable source areas for the studied Dhanjori quartzites.

Table 5. The recovery values (%) of the analytes

Analyte	GSR-4 (CV)	GSR-4 (OV)	SD	Recovery values (%)
Sc	4.20	4.26	0.07	101.45
V	33.00	32.59	0.15	98.77
Cr	20.00	19.92	0.19	99.60
Co	6.40	6.39	0.03	99.91
Ni	16.60	16.85	0.21	101.52
Cu	19.00	19.06	0.15	100.30
Zn	20.00	20.15	0.10	100.76
Ga	5.30	5.43	0.18	102.37
Rb	29.00	28.71	0.07	99.00
Sr	58.00	57.61	0.13	99.33
Y	21.50	20.99	0.08	97.60
Zr	214.00	209.72	1.79	98.00
Nb	5.90	5.77	0.06	97.85
Cs	1.80	1.86	0.05	103.40
Ba	143.00	144.39	2.23	100.97
La	21.00	20.79	0.30	99.02
Ce	48.00	48.11	0.67	100.22
Pr	5.40	5.36	0.08	99.26
Nd	21.00	20.88	0.21	99.42
Sm	4.70	4.68	0.07	99.48
Eu	1.02	1.03	0.02	101.05
Gd	4.50	4.56	0.06	101.41
Tb	0.79	0.79	0.01	99.93
Dy	4.10	4.06	0.03	99.04
Ho	0.75	0.75	0.02	100.02
Er	2.00	1.97	0.02	98.52
Tm	0.32	0.31	0.01	97.63
Yb	1.92	1.92	0.02	100.14
Lu	0.30	0.29	0.00	97.33
Hf	6.60	6.52	0.18	98.77
Ta	0.42	0.41	0.01	98.69
Pb	7.60	7.63	0.03	100.45
Th	7.00	6.87	0.07	98.15
U	2.10	2.08	0.01	99.04

Paleoweathering

The degree of separation of mobile elements (like Ca, Na, & K) against immobile ones (like Al & Ti) depends on the composition and strength of the parent rock, climatic conditions, and time (Nesbitt and Young, 1982). The chemical index of alteration (CIA) by Nesbitt and Young (1982) is utilized to calculate the intensity of chemical alteration of the provenance by the following equation: CIA = [Al_2O_3/(Al_2O_3+CaO*+Na_2O+K_2O)] × 100 in molar proportions CaO* symbolize the Ca of silicate fraction. In the present work, CaO* is rectified by the method of McLennan (1993). According to this method, CaO* is equal to CaO when CaO is lesser than Na_2O and when CaO is greater than Na_2O then CaO* is supposed to be equal to Na_2O. For unweathered rocks, CIA values are <50 to nearly 100 for highly altered products (initial 50 to 60, moderate 60 to 80 and severe >80; Fedo et al., 1995). The studied samples show CIA values ranging from 41.44 to 84.78 (average 69.41) which suggests moderate to intense

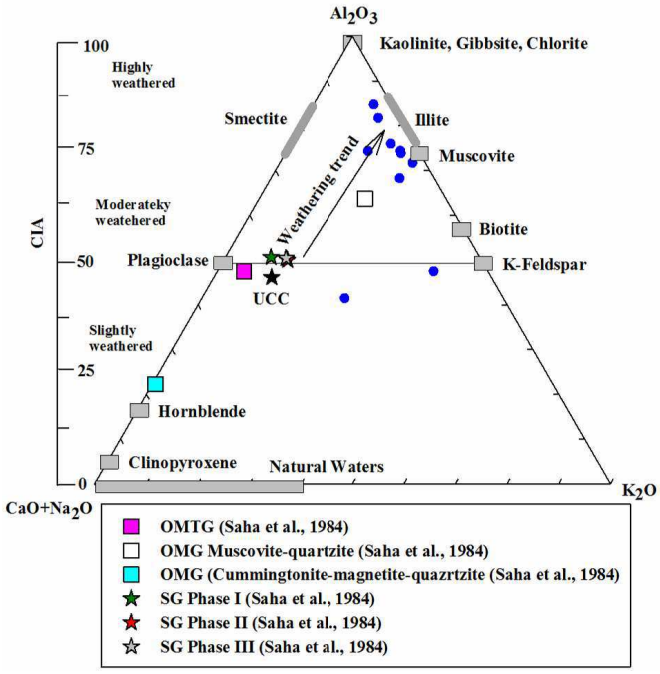

Fig.11. Al_2O_3–(CaO+Na_2O)–K_2O (A–CN–K) diagram for the studied Dhanjori quartzites (after Nesbitt and Young 1984). OMTG: Older metamorphic tonalite gneiss, OMG: older metamorphic group, SG: Singhbhum granite.

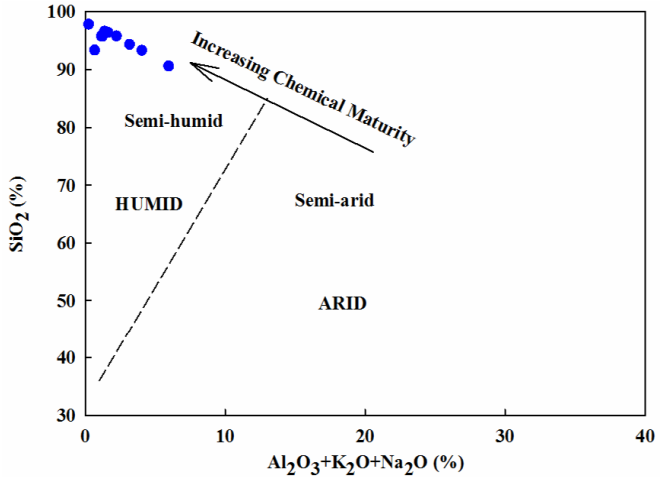

Fig.12. SiO_2 vs. Al_2O_3+K_2O+Na_2O plot for the studied Dhanjori quartzites (Suttner and Dutta, 1986).

weathering conditions (except two samples whose CIA value is less than 50). To note the weathering trends and provenance nature, studied samples have been plotted on a triangular diagram Al_2O_3–($CaO+Na_2O$)–K_2O (A–CN–K) (Nesbitt and Young, 1984). In this diagram, most of the studied samples fall near the Al_2O_3 corner which implies moderate to high degrees of chemical weathering of the provenance (Fig.11). Chemical index of weathering (CIW), which excludes K-metasomatism possibility, is calculated from the equation as $CIW = [Al_2O_3/(Al_2O_3 + CaO^- + Na_2O)] \times 100$ (Harnois, 1988). The studied samples exhibit values of CIW ranging from 57.38 to 96.67 (average 89.19) which further indicates that the source terrain of the studied samples have experienced moderate to severe weathering conditions. Such weathering degrees are also supported by the plagioclase index of alteration $PIA= [(Al_2O_3 – K_2O)/(Al_2O_3 + CaO +Na_2O – K_2O)] \times 100$; (Fedo et al. 1995) which ranges from 30.73 to 95.49 (average 80.15) for the studied samples. Like the CIA, CIW, PIA, and A–CN–K ternary diagram, the Rb/Sr ratio (0.70-7.10) of studied samples too suggests moderate to intense chemical weathering. The strength of chemical weathering depends on the climate and tectonic uplift (Wronkiewicz and Condie, 1987). SiO_2 vs. $Al_2O_3+ K_2O+Na_2O$ plot is used to determine the climatic conditions of the studied Dhanjori quartzites (Suttner and Dutta 1986). The plot shows that the studied Dhanjori Group sediment samples have been derived from a source that has experienced semi-humid climatic conditions (Fig.12). These results corroborate with the conclusions of De et al. (2015). De et al. (2015) have also suggested moderate to severe chemical weathering of the Dhanjori Group.

CONCLUSION

Based on petrography and geochemical character, the studied quartzite samples of Dhanjori Group are categorized into quartz-arenite and sub-arkose. The high quartz abundance of studied samples infers sluggish upliftment in an association of strong weathering of source terrain and deposition in the stable platform. Calculated values of the geochemical indices like CIA, CIW, and PIA infer that the source terrain of the studied samples of the Dhanjori Group have experienced moderate to intense chemical weathering under the humid to semi-humid climatic conditions. In addition to La/Sc, Th/Sc, La/Co, Th/Co ratios, the REE profile showing enrichment in LREE with negative Ce anomalies and flat HREE with negative Eu anomaly indicates the derivation of the sediments for the studied sample of the Dhanjori Group from the mixed source (felsic plus mafic) probably from the OMG, SBGC, and associated Archaean metavolcanic terrains.

Acknowledgements: We are thankful to the Chairman, Department of Geology, Aligarh Muslim University, for providing facilities to carry out this work. We are highly thankful to the Director, NGRI, for permission to analyses of these samples. Last but not least, authors pay sincere thanks to anonymous reviewers for their valuable comments and suggestions without which this work in its present form was not possible. I am also thankful to the University Grant Commission (UGC) India, for financial support, in the form of Maulana Azad National Fellowship (MANF), (No. 201516-MANF-2015-17-UTT-61721).

References

Acharyya, S.K., Gupta, A. and Orihashi, Y. (2010) Neoarchaean–Paleoproterozoic stratigraphy of the Dhanjori basin, Singhbhum Craton, Eastern India: And recording of a few U–Pb zircon dates from its basal part. Jour. Asian Earth Sci., v.39(6), pp.527-536.

Alvi, S.H., Mir, A.R. and Bhat, I.M. (2019) Geochemistry of Dalma metavolcanic Suite from Proterozoic Singhbhum Mobile Belt, Eastern India: Implications for Petrogenesis and Tectonic Setting. Jour. Geol. Soc. India, v.94, pp.351-358.

Armstrong-Altrin, J.S., Lee, Y.I., Verma, S.P. and Ramasamy, S. (2004) Geochemistry of sandstones from the Upper Miocene Kudankulam Formation, southern India: implications for provenance, weathering, and tectonic setting. Jour. Sediment. Res., v.74(2), pp.285-297.

Banerjee, P.K. (1982) Stratigraphy, petrology and geochemistry of some Precambrian basic volcanic and associated rocks of Singhbhum district Bihar and Mayurbhanj and Koenjhar districts, Orissa. Mem. Geol. Surv. India, v.111, pp.58.

Basu, A. (1985) Structure and stratigraphy in and around SE-part of Dhanjori Basin, Singhbhum, Bihar. Rec. Geol. Surv. India, v.113, pp.59-67.

Bhatia, M.R. and Crook, K.A.W. (1986) Trace element characteristics of greywackes and tectonic settling discriminations of sedimentary basins. Contrib. Mineral. Petrol., v.92, pp.181-193.

Bhattacharya, H.N. and Mahapatra, S. (2008) Evolution of the Proterozoic rift margin sediments North Singhbhum Mobile Belt, Jharkhand–Orissa, India. Precambrian Res., v.162, pp.302–316.

Condie, K.C. (1993) Chemical composition and evolution of the upper continental crust: contrasting results from surface samples and shales. Chemical Geol., v.104(1-4), pp.1-37.

Cox, R., Lowe, D.R. and Cullers, R.L. (1995) The influence of sediment recycling and basement composition on evolution of mudrock chemistry in the south-western United States. Geochim. Cosmochim. Acta, v.59(14), pp.2919-2940.

Crook, K.A. (1974) The significance of compositional variation in flysch arenites (graywackes). Lithogenesis and geotectonics, v.19, pp.304-310.

Cullers, R.L., Basu, A. and Suttner, L.J. (1988) Geochemical signature of provenance in sand-size material in soils and stream sediments near the Tobacco Root batholith, Montana, USA. Chemical Geol., v.70(4), pp.335-348.

Cullers, R.L. (2000) The geochemistry of shales, siltstones and sandstones of Pennsylvanian Permian age, Colorado, USA: implications for provenance and metamorphic studies. Lithos, v.51, pp.181-203.

Cullers, R.L. and Podkovyrov, V.N. (2000) Geochemistry of the Mesoproterozoic Lakhanda shales in south eastern Yakutia, Russia: implications for mineralogical and provenance control, and recycling. Precambrian Res., v.104(1), pp.77-93.

Cullers, R.L (2002) Implications of elemental concentrations for provenance, redox conditions, and metamorphic studies of shales and limestones near Pueblo, CO, USA. Chemical Geol., v.191, pp.305-327.

De, S., Mazumder, R., Ohta, T., Hegner, E., Yamada, K., Chiarenzelli, J., Altermann, W., Bhattacharyya, T. and Arima, M. (2015) Geochemistry and Nd isotopic characteristics of the Paleoproterozoic metasedimentary rocks of the Singhbhum Craton and their implications for provenance, paleoclimate and paleo weathering. Precambrian Res., v.256, pp.62-78.

Dickinson, W. R. (1985) Interpreting provenance relations from detrital modes of sandstones. *In:* Provenance of arenites, Springer, Dordrecht, pp.333-361.

Dunn, J.A. and Dey, A.K. (1942) The geology and petrology of Eastern Singhbhum and surrounding areas. Mem. Geol. Surv. India, v.69(2), pp.281-456.

Ekosse, G. (2001) Provenance of the Kgwakgwe kaolin deposit in Southeastern Botswana and its possible utilization. Applied Clay Sci., v.20(3), pp.137-152.

Fedo, C.M., Nesbitt, H.W. and Young, G.M. (1995) Unraveling the effects of potassium metasomatism in the sedimentary rocks and paleosols with implications for paleoweathering conditions and provenance. Geology, v.23, pp.921-924.

Gupta, A., Basu, A. and Singh, S.K. (1985) Stratigraphy and petrochemistry of Dhanjori greenstone belt, Eastern India.The Quart. Jour. Geol. Min. Metall. Soc. India, v.57, pp.248–263.

Gupta, A. and Basu, A. (2000) North Singhbhum Proterozoic mobile belt, Eastern India-A Review. Geol. Surv. India, Spec. Publ., v.55, pp.195-226.

Harnois, L. (1988) The CIW index: a new chemical index of weathering, II Sedimentary Geology, v.55, pp.319-322.

Hayashi, K.I., Fujisawa, H., Holland, H.D. and Ohmoto, H. (1997) Geochemistry of ~1.9 Ga sedimentary rocks from north eastern Labrador, Canada. Geochim. Cosmochim. Acta, v.61(19), pp.4115-4137.

Herron, M.M. (1988) Geochemical classification of terrigenous sand and shales from core or log data. Jour. Sediment. Res., v.58, pp.820-829.

Krishna, A.K., Murthy, N.N. and Govil, P.K. (2007) Multielement analysis of soils by wavelength-dispersive X-ray fluorescence spectrometry. Atomic Soectroscopy-Norwalk Connecticut, v.28(6), pp.202.

Mazumder, R. and Sarkar, S. (2004) Sedimentation history of the

Paleoproterozoic Dhanjori Formation, Singhbhum, India and its implications. Precambrian Res., v.130, pp.267–287.

Mazumder, R. (2005) Proterozoic sedimentation and volcanism in the Singhbhum crustal province, India and their implications. Sediment. Geol., v.176, pp.167–193.

Mazumder, R., Van Loon, A.J., Mallik, L., Reddy, S.M., Arima, M., Altermann, W., Eriksson, P.G. and De, S. (2012) Mesoarchaean–Palaeoproterozoic stratigraphic record of the Singhbhum crustal province, eastern India: a synthesis. Geol. Soc. London, Spec. Publ., v.365(1), pp.31-49.

Mazumder, R., De, S., Ohta, T., Flannery, D., Mallik, L., Chaudhury, T., Chatterjee, P., Ranaivoson, M.A. and Arima, M. (2015) Palaeo-Mesoproterozoic sedimentation and tectonics of the Singhbhum Craton, eastern India, and implications for global and craton-specific geological events. Geol. Soc. London, Mem., v.43(1), pp.139-149.

McLennan, S.M. (1993) Weathering and global denudation. The Jour. Geol., v.101(2), pp.295-303

McLennan, S.M. (2001) Relationships between the trace element composition of sedimentary rocks and upper continental crust. Geochemistry, Geophysics, Geosystems, v.2(4), paper no. 2000GC000109.

Mir, A.R., Balaram, V. and Alvi, S.H. (2011a) Geochemistry of the mafic dykes in parts of the Singhbhum granitoid complex: petrogenesis and tectonic setting. Arabian Jour. Geosci., v.4, pp.933-943.

Mir, A.R., Alvi, S.H. and Balaram, V. (2011b) Geochemistry, petrogenesis and tectonic significance of the Newer Dolerites from the Singhbhum Orissa Craton, eastern Indian shield. Internat. Geol. Rev., v.53(1), pp.46-60.

Mir, A.R., and Alvi, S.H. (2015) Mafic and ultramafic dykes of Singhbhum craton from Chaibasa, Jharkhand, Eastern India: geochemical constraints for their magma sources. Curr. Sci., v.109(8), pp.1399-1403

Mir, A.R., Bhat, Z.A., Alvi, S.H. and Balaram, V. (2015) Geochemistry of black shales from Singhbhum mobile belt, Eastern India: implications for paleo-weathering and provenance. Himalayan Geol., v.36(2), pp.126-133.

Misra, S. and Johnson, P.T. (2005) Geochronological constraints on evolution of Singhbhum mobile belt and associated basic volcanics of eastern Indian shield. Gondwana Res., v.8(2), pp.129-142.

Mukhopadhyay, D. (1976) Precambrian stratigraphy of Singhbhum, the problems and a prospect. Indian Jour. Earth Sci., v.3(2), pp.208-219.

Mukhopadhyay, D. (1988) Precambrian of the Eastern Indian Shield. Perspective of the problems. Mem. Geol. Soc. India, v.(8), pp.2-12.

Mukhopadhyay, D. (2001) The Archaean nucleus of Singhbhum: the present state of knowledge. Gondwana Res., v.4(3), pp.307-318.

Nelson, D.R., Bhattacharya, H.N., Thern, E.R. and Altermann, W. (2014) Geochemical and ion-microprobe U–Pb zircon constraints on the Archaean evolution of Singhbhum Craton, eastern India. Precambrian Res., v.255, pp.412-432.

Nesbitt, H., and Young, G.M. (1982) Early Proterozoic climates and plate motions inferred from major element chemistry of lutites. Nature, v.299, pp.715-717.

Nesbitt, H.W., and Young, G.M. (1984) Prediction of some weathering trends of plutonic and volcanic rocks based on thermodynamic and kinetic consideration. Geochim. Cosmochim. Acta, v.48, pp.1523-1534.

Olierook, H.K., Clark, C., Reddy, S.M., Mazumder, R., Jourdan, F. and Evans, N.J. (2019) Evolution of the Singhbhum Craton and supracrustal provinces from age, isotopic and chemical constraints. Earth-Sci. Rev., v.193, pp.237-259.

Pandey, B.K., Gupta, J.N., Lall, Y. and Mahadevan, T.M. (1986) Rb-Srisochron and Sm-Nd model ages for soda granites from Singhbhum Shear Zone, Bihar and their bearing on crustal evolution. Indian Jour. Earth Sci., v.13(2-3), pp.117-128.

Prabhakar, N. and Bhattacharya, A. (2013) Paleoarchaean partial convective overturn in the Singhbhum Craton, Eastern India. Precambrian Res., v.231, pp.106-121.

Roser, B.P. and Korsch, R.J. (1988) Provenance signatures of sandstone mudstone suites determined using discriminant function analysis of major element data. Chemical Geol., v.67(1-2), pp.119-139.

Roser, B.P. (2000) Whole-rock geochemical studies of clastic sedimentary suites, Mem. Geol. Soc. Japan, v.57, pp. 73–89.

Sarkar, S.N., and Saha, A.K. (1983) Structure and tectonics of the Singhbhum-Orissa iron ore craton, eastern India. In Structure and tectonics of Precambrian rocks. Hindustan Publication Corporation, New Delhi, pp.1–25.

Saha, A.K. (1994) Crustal evolution of Singhbhum-north Orissa, eastern India. Mem. Geol. Surv. India, v.27, p.341.

Sarkar, S.C. and Deb, M. (1971) Dhanjori basalts and some related rocks. Jour. Geol. Min. Metall. Soc. India, v.43, pp.29-37.

Satyanarayanan, M., Balaram, V., Sawant, S.S., Subramanyam, K.S.V., Krishna, G.V., Dasaram, B. and Manikyamba, C. (2018) Rapid determination of REEs, PGEs, and other trace elements in geological and environmental materials by high resolution inductively coupled plasma mass spectrometry. Atomic Spectroscopy, v.39(1), p.1-15.

Singh, S.P. and Nim, S.P. (1998) Stratigraphy of the Lower Proterozoic Sequence of Patharchakri-Mosaboni Area, Singhbhum, Bihar. Indian Minerals, v.52, pp.1-14.

Sunil kumar, T.S., Krishna, Rao, N., Palrecha, M.M., Parthasarthy, R., Shah, V.L. and Sinha, K.K. (1998) Mineralogical and geochemical characteristics of the basal Quartz Pebble Conglomerate of Dhanjori Group, Singhbhum Craton, India and their significance. Jour. Geol. Soc. India, v.51(6), pp.761-776.

Suttner, L.J. and Dutta, P.K. (1986) Alluvial sandstone composition and paleoclimate; I, Framework mineralogy. Jour. Sediment. Res., v.56(3), pp.329-345.

Taylor, S.R. and Mclennan, S.M. (1985) The continental crust: its composition and evolution. Oxford; Melbourne: Blackwell Scientific Publications.

Újvári, G., Varga, A.and Balogh-Brunstad, Z.S. (2008) Origin, weathering, and geochemical composition of loess in south-western Hungary. Quaternary Res., v.69, pp.421–437.

Wronkiewicz, D.J. and Condie, K.C. (1987) Geochemistry of Archaean shales from the Witwatersrand Supergroup, South Africa: source-area weathering and provenance. Geochim. Cosmochim. Acta, v.51(9), pp.2401-2416.

(Received: 31 October 2019; Revised form accepted: 30 October 2020)